

How to avoid a negative shift in reflection-type surface plasmon resonance biosensors with metallic nanostructures

Nak-Hyeon Kim,¹ Tae Woo Kim,² and Kyung Min Byun^{1,*}

¹Department of Biomedical Engineering, Kyung Hee University, Yongin, 446-701, South Korea

²School of East-west Medical Science, Kyung Hee University, Yongin 446-701, South Korea

*kmyun@khu.ac.kr

Abstract: We experimentally demonstrate that introduction of a dielectric film can prevent the surface plasmon resonance (SPR) curve from being shifted to a smaller angle, called negative shift, which occurs unpredictably when metallic nanostructures deposited on a metal film are exposed to an adsorption of binding analytes. From parylene coating experiments, we find that the proposed reflection-type SPR system with a low refractive index MgF₂ film and gold nanorods can provide an enhanced sensitivity by more than 6 times as well as a reliable positive shift. It is due to the fact that use of a dielectric film can contribute to the compensation of an anomalous dispersion relation and the prevention of a destructive interaction of propagating surface plasmons with multiple localized plasmon modes. Our approach is intended to show the feasibility and extend the applicability of the proposed SPR system to diverse biomolecular reactions.

©2014 Optical Society of America

OCIS codes: (240.6680) Surface plasmons; (280.1415) Biological sensing and sensors; (310.6628) Subwavelength structures, nanostructures.

References and links

1. J. Homola, "Present and future of surface plasmon resonance biosensors," *Anal. Bioanal. Chem.* **377**(3), 528–539 (2003).
2. A. Shalabney and I. Abdulhalim, "Sensitivity-enhancement methods for surface plasmon sensors," *Laser Photon. Rev.* **5**(4), 571–606 (2011).
3. X. D. Hoa, A. G. Kirk, and M. Tabrizian, "Towards integrated and sensitive surface plasmon resonance biosensors: a review of recent progress," *Biosens. Bioelectron.* **23**(2), 151–160 (2007).
4. L. He, M. D. Musick, S. R. Nicewarner, F. G. Salinas, S. J. Benkovic, M. J. Natan, and C. D. Keating, "Colloidal Au-enhanced surface plasmon resonance for ultrasensitive detection of DNA hybridization," *J. Am. Chem. Soc.* **122**(38), 9071–9077 (2000).
5. L. A. Lyon, M. D. Musick, and M. J. Natan, "Colloidal Au-enhanced surface plasmon resonance immunosensing," *Anal. Chem.* **70**(24), 5177–5183 (1998).
6. K. M. Byun, S. J. Kim, and D. Kim, "Design study of highly sensitive nanowire-enhanced surface plasmon resonance biosensors using rigorous coupled wave analysis," *Opt. Express* **13**(10), 3737–3742 (2005).
7. K. M. Byun, S. J. Yoon, D. Kim, and S. J. Kim, "Experimental study of sensitivity enhancement in surface plasmon resonance biosensors by use of periodic metallic nanowires," *Opt. Lett.* **32**(13), 1902–1904 (2007).
8. N.-H. Kim, W. K. Jung, and K. M. Byun, "Correlation analysis between plasmon field distribution and sensitivity enhancement in reflection- and transmission-type localized surface plasmon resonance biosensors," *Appl. Opt.* **50**(25), 4982–4988 (2011).
9. S. M. Jang, D. Kim, S. H. Choi, K. M. Byun, and S. J. Kim, "Enhancement of localized surface plasmon resonance detection by incorporating metal-dielectric double-layered subwavelength gratings," *Appl. Opt.* **50**(18), 2846–2854 (2011).
10. E. D. Palik, *Handbook of Optical Constants of Solids* (Academic, 1985).
11. B. J. Jeon, M. H. Kim, and J. C. Pyun, "Application of a functionalized parylene film as a linker layer of SPR biosensor," *Sens. Actuators B Chem.* **154**(2), 89–95 (2011).
12. T. Read, R. V. Olkhov, and A. M. Shaw, "Measurement of the localised plasmon penetration depth for gold nanoparticles using a non-invasive bio-stacking method," *Phys. Chem. Chem. Phys.* **15**(16), 6122–6127 (2013).
13. E. T. Arakawa, M. W. Williams, R. N. Hamm, and R. H. Ritchie, "Effect of damping on surface plasmon dispersion," *Phys. Rev. Lett.* **31**(18), 1127–1129 (1973).
14. R. W. Alexander, G. S. Kovener, and R. J. Bell, "Dispersion curves for surface electromagnetic waves with damping," *Phys. Rev. Lett.* **32**(4), 154–157 (1974).

15. D. Kim, "Effect of resonant localized plasmon coupling on the sensitivity enhancement of nanowire-based surface plasmon resonance biosensors," *J. Opt. Soc. Am. A* **23**(9), 2307–2314 (2006).
16. Y. S. Jung, J. Wuenschell, H. K. Kim, P. Kaur, and D. H. Waldeck, "Blue-shift of surface plasmon resonance in a metal nanoslit array structure," *Opt. Express* **17**(18), 16081–16091 (2009).
17. R. Micheletto, K. Hamamoto, T. Fujii, and Y. Kawakami, "Tenfold improved sensitivity using high refractive-index substrates for surface plasmon sensing," *Appl. Phys. Lett.* **93**(17), 174104 (2008).
18. F. Bahrami, M. Maisonneuve, M. Meunier, J. S. Aitchison, and M. Mojahedi, "An improved refractive index sensor based on genetic optimization of plasmon waveguide resonance," *Opt. Express* **21**(18), 20863–20872 (2013).
19. A. Shalabney and I. Abdulhalim, "Figure-of-merit enhancement of surface plasmon resonance sensors in the spectral interrogation," *Opt. Lett.* **37**(7), 1175–1177 (2012).
20. A. Lahav, M. Auslender, and I. Abdulhalim, "Sensitivity enhancement of guided-wave surface-plasmon resonance sensors," *Opt. Lett.* **33**(21), 2539–2541 (2008).
21. H.-G. Flesch, O. Werzer, M. Weis, J. Jakabovič, J. Kováč, D. Haško, G. Jakopič, H. J. Wondergem, and R. Resel, "A combined X-ray, ellipsometry and atomic force microscopy study on thin parylene-C films," *Phys. Status Solidi A* **206**(8), 1727–1730 (2009).
22. L. Qin, S. Zou, C. Xue, A. Atkinson, G. C. Schatz, and C. A. Mirkin, "Designing, fabricating, and imaging Raman hot spots," *Proc. Natl. Acad. Sci. U.S.A.* **103**(36), 13300–13303 (2006).

1. Introduction

Surface plasmons are transverse magnetic (TM) polarized waves trapped along a metal-dielectric interface. The resonant interaction between surface charge and incident light, called surface plasmon resonance (SPR), is responsible for the collective oscillations of free electrons. Since the SPR signal is sensitive to any variation in the refractive index or the thickness of a sensing medium around a metallic substrate, one can measure the adsorption of target analytes by tracking a change in resonance angle. However, despite several unique advantages of a SPR biosensor, such as rapid, quantitative, and label-free detection, it often suffers from insufficient sensitivity for biomolecules at very low molecular weights [1]. In order to surmount this limitation, there have been a lot of studies for amplifying the SPR signal [2,3]. For example, some researchers proposed the strategy incorporating metallic nanoparticle-labeled target analytes [4,5]. Since the use of metallic nanoparticles can provide a greatly enhanced field-matter interaction as well as an additional refractive index change, the sensor sensitivity was improved by more than an order, compared to a conventional SPR system. On the other hand, tagging biomolecules with colloidal metallic nanoparticles converts a label-free SPR detection into a labeled one and is thus inevitably afflicted with troublesome labeling procedures.

Recently, alternative SPR scheme with metallic nanogratings deposited on a metal film was proposed to improve the sensitivity while maintaining its intrinsic label-free detection [6,7]. In principle, this approach could serve as an effective way to increase a surface reaction area and to generate a highly confined localized surface plasmon (LSP) modes, thereby increasing the field-matter interaction [8]. Nevertheless, critical issue on a negative shift, implying that the resonance angle changes to a smaller angle during the binding events, remains unclear [6].

It has been found from our previous studies that use of gold nanostructures deposited on a thin gold film makes the SPR curve broader and shallower inevitably [9]. When an excitation of LSP mode becomes dominant, especially for extremely fine or densely packed gold nanogratings, the SPR curves are greatly distorted by multiple LSP excitations, often resulting in the negative shift. Although it does not adversely affect the SPR sensing performance as long as the nature of the shift is *a priori* known, the negative shift is unpredictable and is generally accompanied by a notable degradation of SPR signal quality. As a result, it can increase uncertainty in sensor output and high standard errors in measurement.

For those reasons, in this study, we intend to avoid the negative shift while preserving an enhanced sensitivity in SPR detection by incorporating a dielectric film and gold nanostructures. This study will serve as the first step to demonstrate the possibility of guaranteeing a reliable and positive SPR signal amplification as well as the feasibility of improving field-matter interaction for recognizing biomolecular reactions of low molecular weights.

2. Experimental

2-A. Sample Fabrication

Taking account of the advantages of a large-area nanosized pattern, such as robustness to fabrication error and reliability in experiments, we utilized a volatile solvent in distributing gold nanorods on a planar substrate. As shown in Fig. 1, a 45-nm thick gold film was deposited onto an NSF10 glass after an evaporation of a 5-nm thick titanium adhesion layer. A 40-nm thick MgF_2 layer with a low refractive index of $n = 1.384$ at $\lambda = 633 \text{ nm}$ [10] was formed on the gold film via an e-beam evaporation method. Finally, a diluted solution containing gold nanorods was applied to the substrate and then loaded on a hot plate for 10 min to remove the volatile solution. After the processes, the substrate produced a uniform distribution of gold nanorods over a large area. Figure 2 shows the top and cross-sectional view images of the fabricated samples with gold nanorods on a dielectric MgF_2 film using scanning electron microscopy (SEM). Gold nanorods have a rectangular shape of a width of $w = 10 \text{ nm}$ and a length of $l = 30 \text{ nm}$ and a thickness of $h = 10 \text{ nm}$. The total size of gold nanorods pattern was approximately $10 \times 10 \text{ mm}^2$.

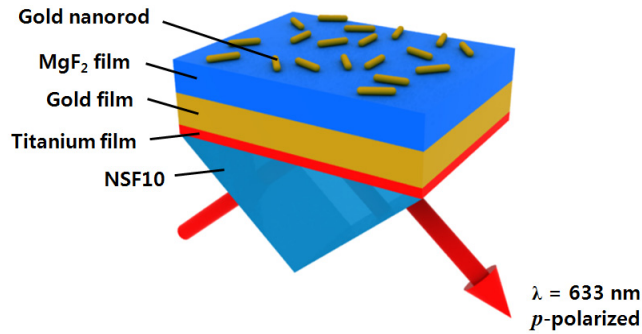


Fig. 1. Schematic of the proposed SPR system incorporating a dielectric film and gold nanorods. A 45-nm thick gold film is evaporated on a NSF10 glass substrate via adhesion of a 5-nm thick titanium layer. MgF_2 film of a low refractive index is then applied as a dielectric layer. Finally, gold nanorods are randomly distributed on top of the fabricated substrate. TM-polarized light with $\lambda = 633 \text{ nm}$ is incident with an angle of θ .

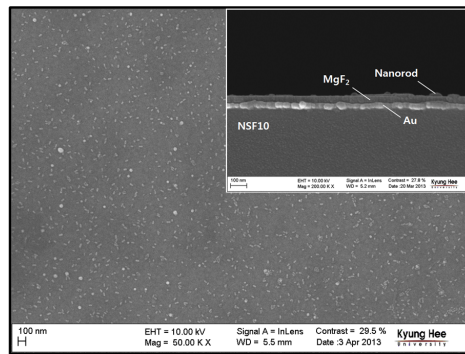


Fig. 2. Top and cross-sectional view SEM images of the deposited gold nanorods on MgF_2 /gold film. The width, length, and thickness of individual gold nanorods are 10, 30, and 10 nm, respectively.

2-B. Optical Measurement Setup

The fabricated samples were measured by a custom-made SPR setup to find a resonance angle. Incident light from a He–Ne laser of $\lambda = 633$ nm was passed through a polarizer to produce a TM mode signal. An optical chopper and a lock-in amplifier were employed to reduce an overall noise level. Reflected light from the sample was calibrated by a photodiode as an optical detector. Our SPR setup was based on dual concentric motorized rotation stages for angle scanning measurement with a nominal angular resolution of 0.002° . During the experiments, SPR curves were measured with a resolution of 0.01° .

2-C. Parylene Film Deposition

To test the sensor sensitivity, a parylene film was applied on the substrates and the sensor sensitivity was estimated by comparing the resonance angles before and after the film deposition. Although the sensitivity obtained from layered biointeractions such as DNA hybridization and protein-protein reaction could be a more practical performance measure, the degree of biomolecular interactions cannot be identical for gold and MgF_2 surfaces as the immobilization efficiency of the ligands varies with the substrate material. On the other hand, a parylene film deposition can reduce such experimental variances. Indeed, a parylene film has been frequently used as a linker layer to promote the covalent immobilization of proteins in SPR biosensing applications [11]. Note that the parylene film thickness was determined to produce an effective field-matter interaction within the penetration depth of plasmon fields [12].

The deposition procedure of a parylene film was as follows: The fabricated SPR samples were carefully rinsed with distilled water. After an evaporation of dimer at 160°C and a pyrolysis process at 650°C , the parylene layer was coated on the substrate at room temperature. The whole process was reproducibly carried out by a microprocessor-controlled parylene coater. The thickness of the parylene film was controlled by the initial amount of parylene dimer at a fixed deposition pressure. Ratio of the thickness to the monomer was measured to be 0.3 nm/mg for parylene-C averaged from four measurements.

3. Results and discussion

Figure 3 shows the reflectance curves of conventional and gold nanorods-based SPR samples when a parylene layer forms a uniform coverage over the sensor substrates. The parylene film thickness measured by atomic force microscopy is obtained to be 4.8 ± 1.2 nm. The solid black and red lines indicate the curves before and after the deposition of parylene film in an air environment. For bare gold film, the resonance angle shifts from 39.17° to 39.40° ; thus, the net change is 0.23° . However, the SPR substrate with gold nanorods exhibits a large negative shift of -1.73° in resonance angle, implying a notable improvement in sensitivity by -7.5 times.

This negative SPR shift is possibly due to a large damping by strong index contrast in the dispersion relation or a phase retardation by the LSP modes excited at gold nanorods. Interestingly, the concept of negative shift was reported as early as in the 1970s, when it was dubbed as back-bending [13,14]. For our experiment based on randomly distributed gold nanorods, damping-related back-bending of plasmon momentum kicks in, which induces the resonance momentum to be smaller with an increasing adsorption, although in a way complicated by the presence of gold nanorods [15]. Jung et al. also demonstrated that the anomalous behavior of surface plasmons can give rise to an exceptional blue-shift in the peak wavelength of a transmission-type plasmonic biosensor with metal nanoslit arrays [16]. Contrary to a typical red-shift in resonance wavelength with an adsorption of a target layer, the blue-shift often occurs by the interplay of anomalous dispersion and multiple LSP modes at the metallic nanostructures.

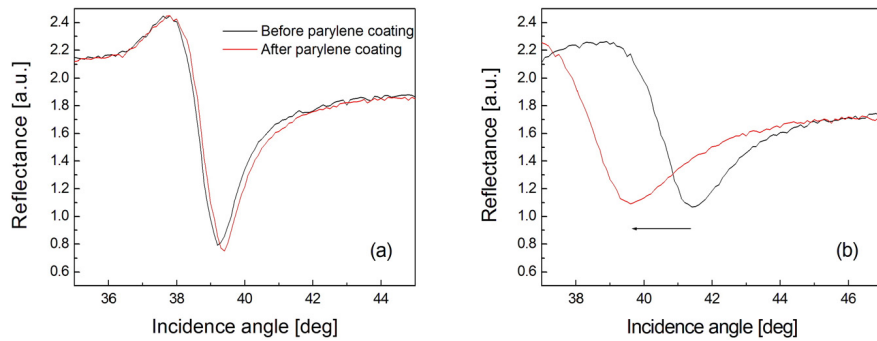


Fig. 3. SPR curves obtained from parylene coating experiments (a) for conventional bare gold substrate and (b) for SPR substrate with gold nanorods. The black and red lines represent the results before and after depositing a parylene film, respectively.

In addition to a negative SPR shift, as destructive coupling of surface plasmon waves with multiple LSP excitations may lead to an adverse effect of degenerated SPR characteristics [9], the reflectance curves in Fig. 3(b) present a broader and shallower resonance band, compared to those in Fig. 3(a). While magnitude of the negative shift is greater than the SPR angle change of a conventional SPR system, degradation of SPR signal quality can increase an uncertainty in measurement and thus aggravate an accurate detection of binding events.

Hence, in order to avoid an unpredictable plasmonic behavior of negative shift and to make the SPR characteristics more reliable, we introduced a dielectric film between a thin gold film and gold nanorods. In our previous numerical studies, periodic gold-SiO₂ double-layered nanogratings were suggested to obtain a positive amplification of the SPR shift [9]. Curve broadening and flattening were also significantly reduced by the use of a SiO₂ spacer. Inspired by previous theoretical insights, we optimized the refractive index and the thickness of a dielectric film and chose a process-compatible MgF₂ layer. While the results are not shown here, dielectric film of low refractive index is apt to realize both a high sensitivity and a wider dynamic range [17].

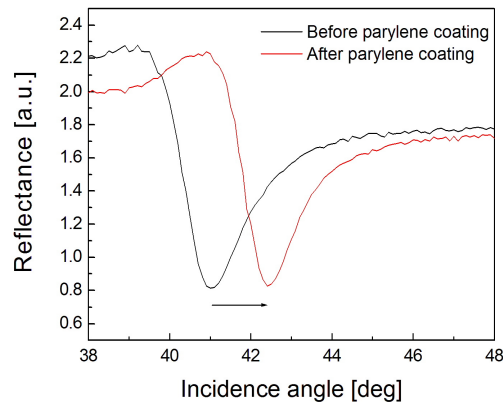


Fig. 4. SPR curves obtained from parylene coating experiments for the proposed SPR substrate with 40-nm thick MgF₂ film and gold nanorods.

Figure 4 shows the measured reflectance curves of the SPR substrate with MgF₂ film and gold nanorods before and after coating a parylene film. There are a few important points worth mentioning: 1) Obviously, resonance angle shift becomes positive according to a refractive index change on a sensor surface. Also, the fabricated SPR substrate exhibits a

large shift of 1.42° , which corresponds to 6.2 times improvement in sensor sensitivity. This enhancement is mainly due to an efficient excitation of LSP modes in the vicinity of gold nanorods and a strong overlap of target matters with the excited LSP modes. 2) A narrower and deeper reflectance curve is achieved, which is due to the fact that a dielectric spacer can make the absorptive damping of surface plasmon waves by gold nanorods less prominent. This effect resembles a dramatic improvement in the SPR signal profile induced by plasmon waveguide resonance (PWR) system with a silica coating evaporated onto a gold film [18]. Sharp resonance profile and large probing depth associated with dielectric waveguide modes of PWR biosensor, which are advantageous especially for detecting large biomaterials such as cells or bacteria, match well an overall trend of the experimental results in Fig. 4.

More samples were additionally tested to verify the consistency of our experimental data. In Fig. 5, the mean values and standard errors in SPR angle shift were determined as $0.22^\circ \pm 0.006^\circ$ for conventional SPR substrates, $-1.62^\circ \pm 0.058^\circ$ for gold nanorod-based ones, respectively. Thus, the sensitivity enhancement factor (SEF), defined as the ratio of $\Delta\theta_{\text{SPR}}$ for conventional system to $\Delta\theta_{\text{SPR}}$ for SPR system with MgF_2 film or gold nanorods, was measured to be -7.4 . On the other hand, SPR substrates with gold nanorods and MgF_2 film exhibited a positive shift of $1.45^\circ \pm 0.062^\circ$, implying a SEF value of 6.6. Spatial variances in nanorod distribution are responsible for relatively high experimental errors in the sensitivity results.

It should be also emphasized that the added MgF_2 layer can contribute to not only prevention of negative shift but enhancement of sensitivity. While the SPR curves are not shown here, resonance angle shift of SPR substrates with a 40-nm thick MgF_2 film was found to be $0.38^\circ \pm 0.023^\circ$, which indicates an $\text{SEF} = 1.7$. It was previously addressed that by adding a very thin dielectric layer of a high refractive index on top of a metallic film, the sensor sensitivity can be considerably improved due to an enhanced plasmon fields at the analyte interface [19,20]. The obtained SEF in this study is not substantial as expected because MgF_2 layer has a relatively low refractive index [21] and its thickness is not the optimum for high sensitivity. However, in subsequent studies, further optimization of the thin dielectric layer and its combination with various gold nanostructures could lead to a significant improvement of the figure-of-merit in overall sensor performance as well as the sensitivity.

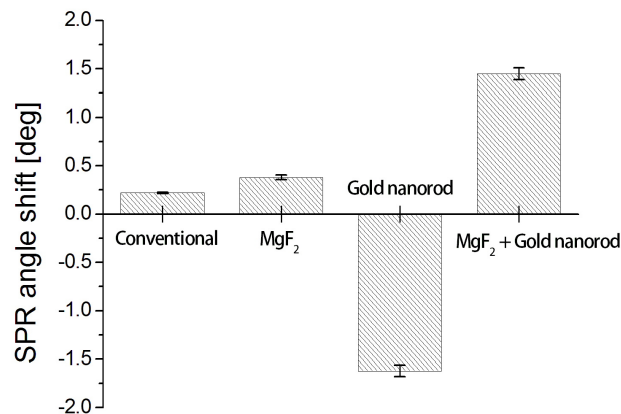


Fig. 5. Statistical data of the SPR angle shift of four different samples for parylene coating experiments. The average resonance shifts and the errors are determined to be $0.22^\circ \pm 0.006^\circ$ for conventional SPR substrate, $0.38^\circ \pm 0.023^\circ$ for MgF_2 -based one with an $\text{SEF} = 1.7$, $-1.62^\circ \pm 0.058^\circ$ for gold nanorod-based one with a negative $\text{SEF} = -7.4$. The SPR substrate with MgF_2 film and gold nanorods exhibits a positive shift of $1.45^\circ \pm 0.062^\circ$, yielding a $\text{SEF} = 6.6$.

Finally, in order to verify the effect of MgF_2 layer, we intend to visualize the enhanced plasmon fields near the SPR surface using the finite-difference time-domain (FDTD) method. The minimum grid size for the FDTD was set to be 0.5 nm. For comparison study, we have chosen conventional and gold nanograting-mediated SPR substrates with and without a 40-nm-thick MgF_2 spacer. Note that, we use a periodic gold nanograting model with a period of 100 nm, a width of 10 nm and a depth of 10 nm to simplify the randomly distributed gold nanorods. While gold nanograting model is not exactly consistent with gold nanorod, this can give us a hint that dielectric film can be beneficial for effective excitation of LSP modes. The FDTD calculation in Fig. 6 exhibits well-known features of LSP modes excited by gold nanogratings. Contrary to conventional SPR substrate, the field amplitude reaches a maximum at individual corners of gold nanograting and falls exponentially along the z-axis [22]. More interestingly, two LSP modes in the vicinity of lower corners of gold nanograting in Fig. 6(b) are not efficiently excited, which is probably attributed to a destructive interaction of the LSP modes with a thin gold film. On the other hand, we can confirm in Fig. 6(c) that MgF_2 layer plays a key role in preventing LSP modes from being degenerated, therefore improving a field-matter interaction at substrate-analyte interfaces.

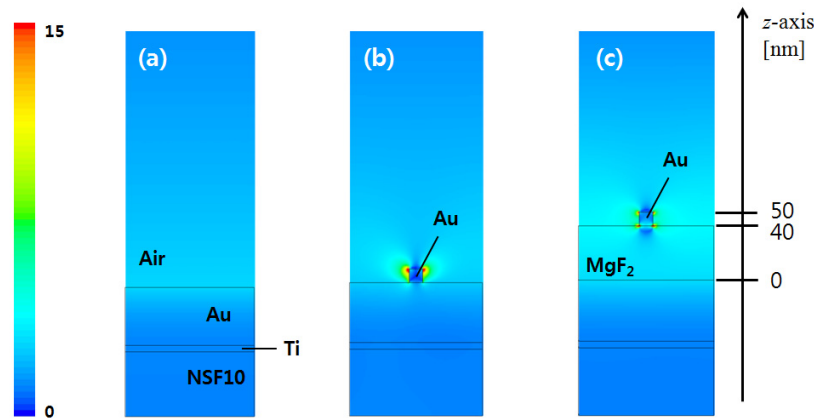


Fig. 6. FDTD results of SPR substrates with (a) a bare gold film, (b) gold nanograting on gold film, and (c) gold nanograting on MgF_2 /gold film. Gold nanograting has a dimension of a width = 10 nm and a depth = 10 nm. Two-dimensional FDTD images are normalized by the field amplitude of 15.

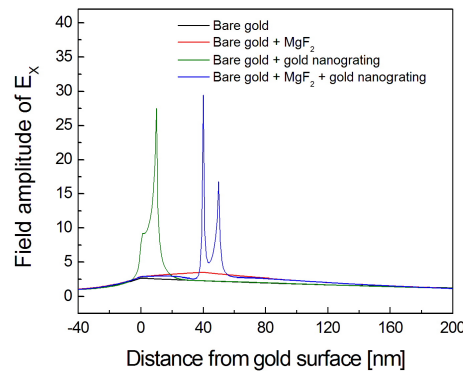


Fig. 7. Vertical E_x field amplitude profiles at the point where maximum field is found for the four different substrates.

Figure 7 shows the vertical amplitude profiles at the point where maximum field of E_x is found. On the assumption that the electric field of an incident beam is of unit amplitude, maximum E_x field amplitudes are obtained as 2.7 for conventional thin-film-based SPR substrate and 3.5 for the one with MgF_2 film. This contrast is associated with a slight increase in sensitivity of MgF_2 -mediated SPR samples. On the other hand, the peak E_x field amplitude is calculated as 27.4 for the SPR substrate with gold nanogratings and 29.5 (the main peak) and 16.8 (the second peak) for the one with gold nanogratings and MgF_2 film. Such efficient LSP excitations of higher amplitudes support an assertion that a dielectric layer contributes to reducing a direct coupling between surface plasmons and LSP modes, resulting in blocking the negative shift and improving the sensor sensitivity simultaneously.

4. Conclusion

In this study, we proposed the SPR substrates with MgF_2 dielectric film between a gold film and gold nanorods to avoid an unpredictable behavior of negative shift in a sensitive plasmonic biosensor. The experimental results presented that combination of MgF_2 dielectric film and gold nanorods can provide a reliable SPR shift to a higher angular momentum as well as better SPR signal and improved sensitivity by more than 6 times. This is attributed to the compensation of an anomalous dispersion relation and the prevention of destructive interplay of surface plasmons with multiple LSP modes. Such a plasmonic interpretation was in good agreement with the numerical analyses based on FDTD computation. Considering rapid advances in surface immobilization and modification techniques, we envision that true realization of the proposed substrate and its applications to a sensitive detection for biomolecular reactions of low molecular weights will be readily feasible.

Acknowledgments

This work was supported by Korea Science and Engineering Foundation (KOSEF) grant funded by the South Korean government (MEST) (2011-0029485) and (NSF-2013R1A1A1A05011990). Tae Woo Kim acknowledges the support by the National Research Foundation of Korea (NRF) grant funded by the South Korean government (MEST) (No. 2013R1A2A2A04016066).